Journal of Catalysis **200,** 79–90 (2001)
doi:10.1006/jcat.2001.3182, available online at http://www.idealibrary.com on IDEAL®

A DFT Study of the Cracking Reaction of Thiophene Activated by Small Zeolitic Clusters

Xavier Rozanska,*,[1] Rutger A. van Santen,* and François Hutschka†

*Schuit Institute of Catalysis, Laboratory of Inorganic Chemistry and Catalysis, Eindhoven University of Technology, P.O. Box 513, 5600 MB Eindhoven, The Netherlands; and †TotalFina, Centre Européen de Recherche et Technique, Procédés et Raffinage, B.P. 27, 76700 Harfleur, France

Received August 29, 2000; revised December 14, 2000; accepted January 15, 2001; published online April 11, 2001

A theoretical study of the cracking reaction of thiophene by small zeolitic cluster catalysts is reported. Cluster density functional theory calculations have been performed. It is shown that cracking of thiophene is catalyzed by Lewis basic oxygen atoms. Several active sites are proposed and tested. Moreover, it appears that the use of a partner molecule, strongly adsorbed to the acidic proton, allows for an important decrease of the cracking activation energy barrier. The effect of hydrogenation of thiophene prior to the cracking reaction has been checked. Interestingly, hydrogenation does not affect dramatically the activation energy barrier (−10 kJ/mol). However a large stabilization of the product of the reaction has been found (−40 kJ/mol). © 2001 Academic Press

Key Words: **Brønsted acid site; zeolite; DFT calculations; quantum chemistry; transition state; desulfurization; cracking.**

1. INTRODUCTION

Severe environmental regulations reduced the minimum specifications for sulfur concentration in fuel (1). There is an interest in studying desulfurization on acidic catalysts. Theoretical studies of the cracking reaction of thiophene, which is used as a test molecule to measure rates of desulfurization (2), are reported to understand acidic catalyst hydrodesulfurization.

Recently, Saintigny *et al.* performed a density functional theory (DFT) study of the desulfurization reaction of thiophene catalyzed by the zeolitic cluster $H_3SiOHAl(OH)_2OSiH_3$, also called 3TOH (3). They investigated a cluster approach method in order to investigate the reaction energy diagram of this reaction (4). Following earlier leads of Garcia and Lercher (5) and the experimental evidence of Welters *et al.* (6), their objective was to understand the mechanism of this reaction. They investigated the thiophene desulfurization reaction in the presence and absence of H_2 and established that H_2 is an important reactant for the reaction to be achieved.

Acidic zeolite catalysts are used in cracking, isomerization, transalkylation, or alkylation reactions (7), and also in hydrotreating reactions (8). Actually, in the case of the hydrodesulfurization reaction, pure acidic zeolites are not used as catalysts. They are part of bifunctional catalysts. The industrial hydrodesulfurization catalysts are γ-alumina supported transition metal sulfides, containing a Mo (or W) disulfide phase promoted by Co (or Ni) (1, 9). Until recently, acidic supports were avoided because they were thought to lead to a deactivation of the active sites by coke formation and also to cracking reactions, reducing the octane rating of the resulting fuel (10). But it is now well established that an acidic zeolite support allows an enhanced activity of the deep desulfurization reaction (6, 11).

Moreover, it has been shown that prehydrogenation of thiophenic aromatic species greatly enhances the desulfurization reaction rates (11, 12). In particular, Yu *et al.* (12c), using alkane as hydrogen source and thiophene as acceptor for this hydrogen, described a significant improvement of the thiophene desulfurization yield when the reaction was catalyzed by acidic zeolite.

In the following, we will focus on the cracking reaction of thiophene. This step has been shown to be an energetically demanding step of the thiophene desulfurization reaction catalyzed by a 3TOH zeolitic cluster (3). This cracking reaction leads to the formation of a thiol alkoxy species. This intermediate is not very stable and undergoes transformation to butadiene-thiol with the help of H_2. Thiol species are not difficult to desulfurize (12). First this cracking reaction catalyzed by an acidic zeolite small cluster model will be extensively described. The mechanism of this reaction step will be analyzed. This analysis leads us to question the structure of the catalytically active site. Several active sites are proposed that may ease the activation of this reaction and are computationally tested. Thiophene is a medium size molecule that can fit without difficulty into medium size pore zeolite catalysts. There is no steric hindrance, which

[1] To whom correspondence should be addressed. Fax: +31 40 245 5054. E-mail: tgakxr@chem.tue.nl.

0021-9517/01 $35.00
Copyright © 2001 by Academic Press
All rights of reproduction in any form reserved.

makes the use of the cluster approach useful for a comparison of activation barrier energies and mechanisms.

2. METHODS

Within the cluster approach, the catalytically active site model system is a small neutral zeolite fragment, terminated with hydrogen atoms or hydroxyl groups. This cluster aims to represent the Brønsted acid site, in interaction with thiophenic species. Such a methodology has been extensively used in the literature to study reactions where proton activation is involved (3, 4). No constraints have been used for the cluster and molecules in interaction with, as recommended before (4e, 13). A tetrahedral T_4 cluster ($Al(OSiH_3)_2(OHSiH_3)(OH)$) has been mainly chosen for our studies. Incidentally, other clusters with four tetrahedral units have also been used (see Results and Discussion).

As the zeolite catalyst is only described by the Brønsted acid site, adsorption energies computed here correspond only to a fraction of the adsorption energies. It is missing all energy contributions of molecules with atoms of the zeolite wall. Therefore, the adsorption energies we present actually describe the affinity of molecules for the Brønsted acid site. It has been discussed elsewhere how to correct empirically the adsorption energies (14).

Moreover, the zeolite framework electrostatic contribution is missing. This can influence the activation energy significantly. Because our study is limited to the very first step of the desulfurization reaction of thiophene, one may assume that the relative differences obtained for the activation energies are conserved when a more realistic model is used. It has been observed that framework contributions can decrease activation energies by 15 to 30% (15). The framework stabilization of charged or transient species appears to be uniform for a given zeolite topology and a given reactant size (16).

Calculations have been performed with Gaussian98 (17) using the density functional method B3LYP (18). This DFT method is a hybrid method which uses a Hartree–Fock core and a Becke exchange functional (18a, c) with the correlation functionnals developed by Lee, Yang, and Parr (18b). Zygmunt *et al.* (19) have shown that this method constitutes the best choice for DFT treatment of zeolite systems.

Basis set d95 has been used in order to make possible comparison with previous results (3). The basis set superposition error (BSSE) correction has been computed on intermediates and transition states using the counterpoise method (20). Quantum chemistry codes like Gaussian98 use basis sets to describe electrons. These basis sets are incomplete but convenient models. Due to the incompleteness of basis sets, when two molecules or molecular fragments A and B are in interaction, electrons of A use basis sets of B and vice versa. This leads to an overestimation of the interaction energy between A and B. BSSE can be estimated and corrected using, for instance, the counterpoise method. The BSSE correction for A–B interaction is given by

$$\Delta_{CP}E(AB) = (E_A(A) - E_A(AB)) + (E_B(B) - E_B(AB)), \quad [1]$$

where $E_X(Y)$ is the energy of system X using basis sets of system Y. The geometries of A and B are the same as those for the A–B system. Once the BSSE has been computed, one has to add this value to the energy of the system in order to obtain the BSSE corrected energy. In the case of transition states it can be impossible to define independent molecular fragments and BSSE is then impossible to compute (20c). This happens for some of the transition states in this study. Therefore, BSSE have been computed but energies are not BSSE corrected. BSSE corrected activation energy is obtained from the relation

$$\Delta_{CP}E_{act} = \Delta_{CP}E_{TS} - \Delta_{CP}E_{ads}, \quad [2]$$

where $\Delta_{CP}E_{TS}$ is the BSSE correction for the transition state energy and $\Delta_{CP}E_{ads}$ the BSSE correction for the ground state energy.

Geometry optimization calculations have been carried out to obtain a local minimum for reactants, adsorption complexes, and products and to determine the saddle point for transition states (TS). The frequencies were computed using analytical second derivatives in order to check that the stationary point exhibits the proper number of imaginary frequencies: none for a minimum and one for a transition state (first-order saddle point). Zero-point energy (ZPE) corrections have been calculated for all optimized structures. All energies presented hereafter are zero-point energies.

3. RESULTS AND DISCUSSION

3.1. Thiophene Cracking Reaction

In this section, we describe the cracking reaction of thiophene catalyzed by a small cluster that models an acidic zeolite catalyst active site. This reaction leads from thiophene to buta-1,2-diene-thiol alkoxy. Civalleri *et al.* (21) stressed recently that the B3LYP method shows a significant basis set dependence, even though it is one of the methods that shows better agreement with experimental data for zeolite systems. We computed the BSSE values for intermediates and transition states (see Table 1). BSSE values obtained with basis set d95 on intermediates and transition states are very reasonable (19, 21).

Only the η^1(S) adsorption mode of thiophene with respect to the acidic proton has been considered in this study. It has been proven experimentally to correspond to the

TABLE 1

Adsorption Energies and Energies, Free Energies, Free Enthalpies, and Entropies of Activation of the Cracking Reaction of the Thiophenic Ring [a]

Molecules	Catalyst	Reaction	E_{ads}(ZPE) (kJ/mol)	E_{act}(ZPE) (kJ/mol)	$\Delta_{298}H_{act}$ (kJ/mol)	$\Delta_{298}G_{act}$ (kJ/mol)	$\Delta_{298}S_{act}$ (J/mol/K)	$\Delta_{ZPE}E$ (alkoxy-ads) (kJ/mol)
Thiophene	H-cluster	(1)	−18(+6)	226(+8)	224	242	−60	108
Thiophene	D-cluster	(2)	−14(+6)	226(+8)	224	242	−60	—
Thiophene	Cluster (charged)	(3)	−21(+6)	197(+6)	196	205	−31	136
Thiophene	CH_3-cluster	(4)	−5	240	241	252	−35	44
Thiophene	Li-cluster	(5)	−32(+8)	205(+8)	203	228	−10	136
Thiophene-H_2S	H-cluster	(6)	−38(+12)	219	219	231	−40	123
Thiophene-H_2O	H-cluster	(7)	−86(+20)	202	200	211	−38	—
Dihydrothiophene	H-cluster	(8)	−38(+8)	214(+8)	212	224	−40	70
Tetrahydrothiophene	H-cluster	(9)	−41(+9)	237(+7)	235	246	−36	79

[a] The differences in energy for all reactions between reactant and product (alkoxy species) are also shown. Values in parentheses for E_{ads} and E_{act} are BSSE corrections in (kJ/mol).

more stable adsorption mode for adsorption of thiophene within the acidic zeolite (5). In this study, it has also been found that the η^1(S) adsorption mode is slightly more favorable than the η^2(CC) adsorption mode ($\Delta E_{ads} \sim 1$ kJ/mol). The adsorption energy of thiophene is $E_{ads} = -18$ kJ/mol (see Table 1). This adsorption energy is low and does not correspond to the experimentally found adsorption energy of thiophene on a Brønsted acidic within a zeolite micropore (see Method) (14).

The activation barrier energy of the thiophene cracking reaction step is 226 kJ/mol (Reaction (1), see Fig. 1 and Tables 1 and 2). The visualization of the imaginary frequency of vibration (i.e., the negative frequency of vibration) that characterizes the saddle point on the potential energy surface and the mechanism involved in this reaction step seems to indicate that the zeolite proton is not directly involved in this reaction step (see Fig. 2). The replacement of this proton by its isotope ^{2}H should change the zero-point activation energy if it participates in the transition state mechanism. The deuterium acidic site (Reaction (2)) gives an activation similar to E_{act} computed for Reaction (1) (see Table 1).

TABLE 2

Geometries of the Transition State Mechanisms for Reactions as Labels Defined in Table 1[a]

	Reaction (1)	Reaction (3)	Reaction (4)	Reaction (8)	Reaction (9)
AlO_1	1.78	1.74	1.90	1.89	1.88
AlO_2	1.76	1.83	1.83	1.84	1.81
AlO_3	1.76	1.75	1.72	1.71	1.71
H_aS	2.33	—	—	2.14	2.03
C_1C_2	1.37	1.36	1.43	1.51	1.50
O_1H_a	1.01	—	—	1.03	1.06
SC_1	2.59	2.61	2.65	2.76	2.83
SC_4	1.76	1.75	1.71	1.81	1.89
C_1O_2	1.85	1.95	1.92	1.87	2.09
SC_1O_2	148.7	165.3	166.7	171.8	127.5
AlO_2C_1	101.9	118.4	71.4	99.0	103.1
C_1SC_4	81.5	81.9	81.9	73.5	81.0
O_1H_aS	176.0	—	—	171.8	167.8
$C_1C_2C_3C_4$	6.5	0.0	−2.9	−25.4	−66.2
$SC_4C_2C_1$	−1.1	1.4	−1.5	−26.3	−9.8

[a] The atom labels are defined in the corresponding pictures of the reactions (Figs. 1, 4 and 8).

The nonparticipation of the acidic proton in the cracking mechanism step is more convincingly shown when a deprotonated cluster is used to catalyze this reaction (Reaction (3), see Tables 1 and 2). This deprotonated cluster is an extreme situation that will not occur experimentally: the energy cost to separate the proton from the cluster with our T_4 cluster is $E_{dep} = 1313$ kJ/mol. However, the use of such a cluster confirms that the acidic proton does not participate in the transition state ($E_{act} = 197$ kJ/mol for Reaction (3), see Figs. 1 and 3). Comparison of the transition state structures of Reaction (1) and Reaction (3) shows the induced differences in thiophene geometry when the proton is present. The thiophene ring orients itself in closer interaction with the cluster in the case of Reaction (1), with the induced negative charge on the sulfur atom being stabilized partially by the acidic proton (distance $H_aS = 2.33$ Å). This interaction brings about a deformation of the thiophene ring (dihedral angle $C_1C_2C_3C_4 = 6.5°$) whereas for Reaction (3) this deformation does not occur (dihedral angle $C_1C_2C_3C_4 = 0.0°$). This may partially explain the difference in activation barrier energies shown between the two cracking steps. The acidic behavior of the Brønsted acidic site is not required to achieve this reaction. For instance, a methyl alkoxy species, not displaying a strong acidic characteristic (the energy of formation of the methyl alkoxy species is $E_{alkoxy,\ release} = 839$ kJ/mol), can successfully break the thiophenic ring (Reaction (4), see Figs. 4 and 5 and Tables 1 and 2). In this case, the activation energy is 240 kJ/mol.

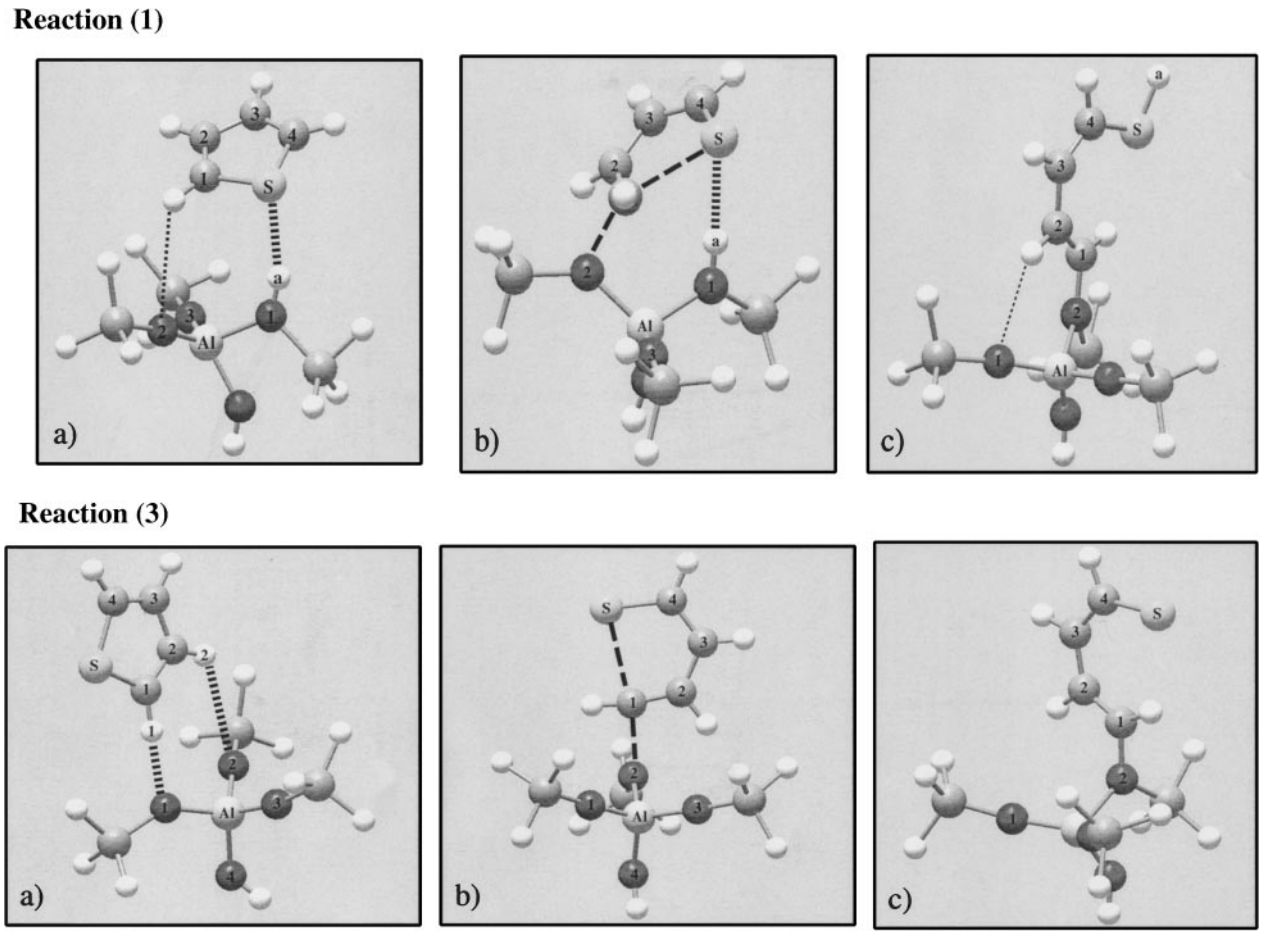

FIG. 1. Geometries of the intermediates (a, c) and transition state (b) of the cracking reaction of thiophene catalyzed by an acidic T_4 cluster $Al(OHSiH_3)(OSiH_3)_2(OH)$ modeling the active Brønsted site of an acidic zeolite catalyst (Reaction (1)) and by a deprotonated T_4 cluster $Al(OSiH_3)_3(OH)$ (Reaction (3)).

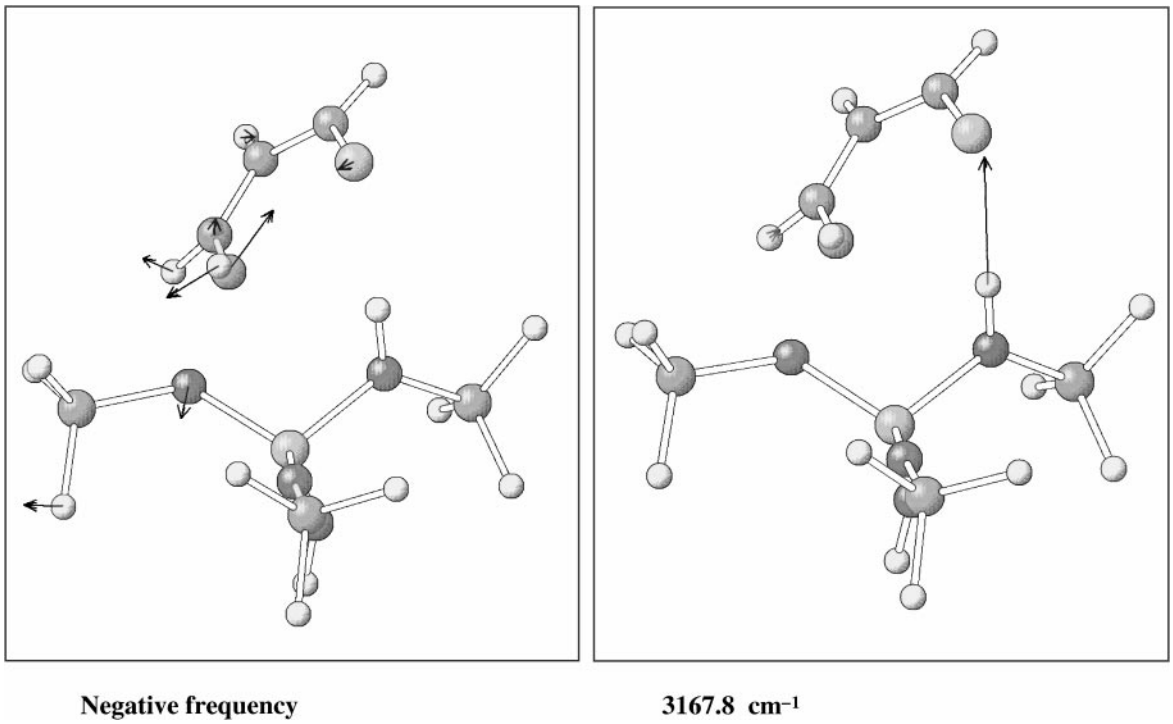

FIG. 2. Visualizations of the imaginary frequency involved in the thiophenic ring cracking transition state of thiophene catalyzed by an acidic T_4 cluster (left) and of the more intense frequency of vibration of this transition state with its calculated value (in cm^{-1}) (right) (Reaction (1)).

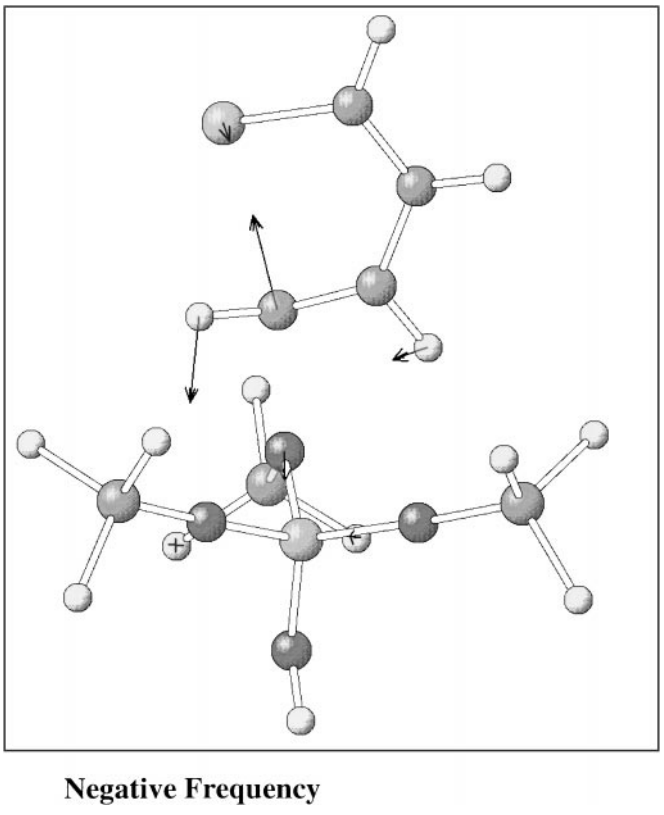

FIG. 3. Visualization of the imaginary frequency involved in the thiophenic ring cracking transition state of thiophene catalyzed by a charged deprotonated T_4 cluster (Reaction (3)).

This is only 14 kJ/mol higher than the activation energy obtained for Reaction (1). This may explain the fast deactivation by coke formation of the thiophene desulfurization reaction catalyzed by acidic zeolite catalysts as observed by Welters *et al.* (6a). Thiophene undergoes as easily a reaction to butadiene-thiol alkoxy as to bigger alkoxy species.

Saintigny *et al.* (3) used in their study a smaller cluster than that used in the present case. The smaller cluster has a higher intrinsic acidity than the one used in this study (deprotonation energies are $E_{dep} = 1329$ and 1313 kJ/mol, respectively). It is well known that E_{act} varies linearly as a function of the deprotonation energy (14b). However, Saintigny *et al.* found an activation energy of 222 kJ/mol for the cracking reaction of thiophene. In the present study we found 226 kJ/mol. This small variation of E_{act} as a function of E_{dep} indicates again that the acidity can be considered not a key factor in this reaction step.

In order to go further in the investigation of the absence of the effect of acid strength on the thiophene cracking reaction, the case of the reaction catalyzed by a Li-exchanged zeolite has been considered (Reaction (5)). Ono (22) and Yu *et al.* (12c) have shown that cation-exchanged zeolites can induce the thiophene cracking reactions. In particular, Ono pointed out that alkali metal-exchanged zeolites catalyze the thiophene-to-furan reaction: one of the intermediates of this reaction has been identified as the same butadiene-thiol alkoxy species as that obtained for the thiophene cracking reaction. In our calculations, we used a T_4 Li-exchanged zeolitic cluster: the Li cation interacts with two Brønsted site oxygen atoms ($LiO_1 = LiO_2 = 1.81$ Å). Thiophene has been considered to interact with the Li atom via the sulfur atom (SLi = 2.61 Å) (see Fig. 6 and Table 3). The adsorption energy is $E_{ads} = -32$ kJ/mol (see Table 1). As in the previous transition states, the cleavage of a thiophene C–S bond is induced by a Lewis basic oxygen atom (see Figs. 6 and 7). Compared with the adsorbed state, the distance LiS becomes shorter in the transition state (SLi = 2.55 Å), whereas the Li–oxygen atoms bonds weaken ($\Delta LiO_1 = \Delta LiO_2 = 0.10$ Å). The thiophene ring atoms remain almost coplanar ($SC_4C_2C_1 = -2.3^\circ$ and $C_1C_2C_3C_4 = 5.1^\circ$). The activation energy of this reaction step is 205 kJ/mol with respect to adsorbed thiophene. This activation energy is comparable with E_{act} of Reaction (3) and 21 kJ/mol lower than E_{act} of Reaction (1). This reaction step leads to the formation of an alkoxy complex in which the Li atom is shared by the sulfur atom (SLi = 2.39 Å) and by two Brønsted site oxygen atoms ($LiO_1 = LiO_2 = 2.00$ Å) (see c in Fig. 6). The energy level of this complex is 136 kJ/mol with respect to adsorbed thiophene. The alkoxy species that is formed when the Li atom is released from the oxygen atoms is considerably less stable ($E = 239$ kJ/mol) (see d in Fig. 6). One should note that for this alkoxy species the distance SLi is 2.26 Å and the Li atom interacts with a C=C bond ($LiC_3 = 2.35$ Å and $LiC_4 = 2.25$ Å) (see Table 3).

The cracking reaction of thiophene appears to be catalyzed by a Lewis basic site. The presence of the Brønsted acidic site proton allows for the "neutralization" of the

TABLE 3

Geometries of the Intermediates and Transition State for the Reaction Catalyzed by Li-Zeolite (Reaction (5)) [a]

(a)		(b)		(c)		(d)	
AlO_1	1.82	AlO_1	1.79	AlO_1	1.76	AlO_1	1.71
AlO_2	1.82	AlO_2	1.79	AlO_2	1.76	AlO_2	1.71
AlO_3	1.73	AlO_3	1.82	AlO_3	1.89	AlO_3	1.90
O_1Li	1.83	O_1Li	1.93	O_1Li	2.00	O_3C_1	1.42
O_2Li	1.83	O_2Li	1.93	O_2Li	2.00	LiS	2.26
LiS	2.61	LiS	2.55	LiS	2.39	LiC_3	2.35
AlLiS	172.9	C_1C_2	1.37	O_3C_1	1.47	LiC_4	2.25
$LiSC_1$	94.6	SC_1	2.57	O_1LiS	123.9	SC_4	1.80
$LiSC_4$	98.2	SC_4	1.77	O_2LiS	140.3		
		C_1O_3	1.91	SC_4	1.79		
		SC_1O_3	151.5				
		AlO_3C_1	100.8				
		C_1SC_4	81.9				
		$C_1C_2C_3C_4$	5.3				
		$SC_4C_2C_1$	−2.3				

[a] The atom labels are defined in the corresponding picture of the reaction (Fig. 6).

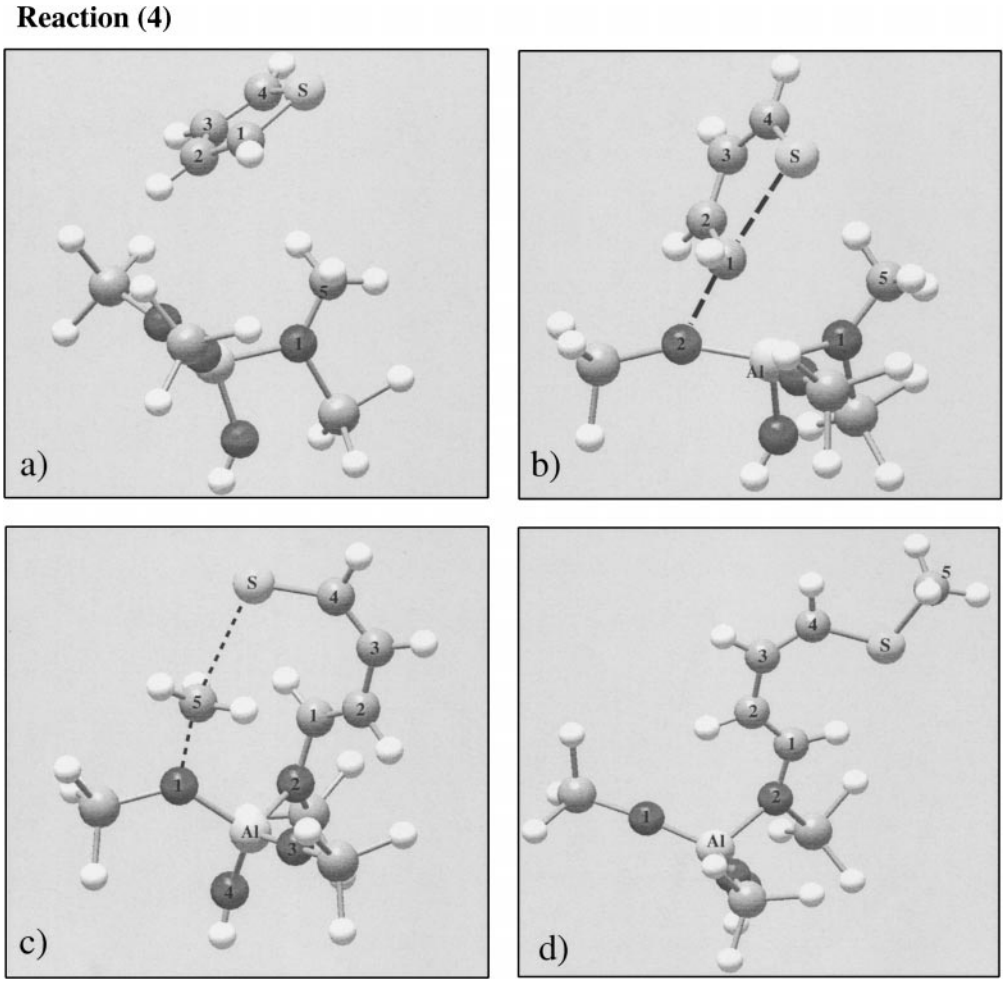

FIG. 4. Geometries of the intermediates (a, d) and transition state (b, c) of the cracking reaction of thiophene catalyzed by a methyl alkoxide cluster (Reaction (4)). Between b and c a transient zwitter-species exists but transforms easily to neutral species d (the activation energies for the backward and forward mechanisms are around 40 and 50 kJ/mol respectively).

consecutively formed charged alkoxy species. No charged intermediate nor protonated transition state could be found. This is in agreement with experimental (23) and theoretical (15a) data. It is well known that acidic zeolite catalysts are not strong enough to allow for the existence of charged aromatic species. Furthermore, cation-exchanged or hydrocarboxy zeolites have been shown to catalyze this reaction. In the case of Li-exchanged zeolitic cluster, the activation energy is around 20 kJ/mol lower than for the reaction catalyzed by an acidic zeolitic cluster, whereas in the case of a methoxy zeolitic cluster it is around 15 kJ/mol higher.

3.2. Assisted Cracking Reaction

It is now established that the thiophene cracking reaction requires mainly the acidic proton as a cation source. The distortion of the thiophenic ring to allow its sulfur atom to be in close interaction with this proton appears to increase the activation barrier energy. One way to overcome this costly distortion is to use external molecules. An external molecule can assist the protonation of sulfur and avoid the distortion of thiophene. H_2O and H_2S will be used for this purpose (Reaction (6) and Reaction (7), see Figs. 8 and 9, and Tables 1 and 4).

In both cases of the optimized geometries of the thiophene-H_2S or -H_2O coadsorbed complex, H_2S and H_2O adsorb strongly to the acidic proton and one of their hydrogen atoms points toward a thiophene C=C bond. Neither H_2S nor H_2O is protonated by the acidic proton of the cluster. The adsorption energies of these complexes are larger than the adsorption energy of thiophene (E_{ads} is -38 and -86 kJ/mol respectively for H_2S and H_2O). These values are very close to the adsorption energies of H_2S and H_2O alone ($E_{ads} = -38$ and -88 kJ/mol respectively). Formation of the complex thiophene-H_2S or thiophene-H_2O is not preferred to the adsorption of only H_2S or H_2O to the cluster. This appears to be in agreement with the experimental

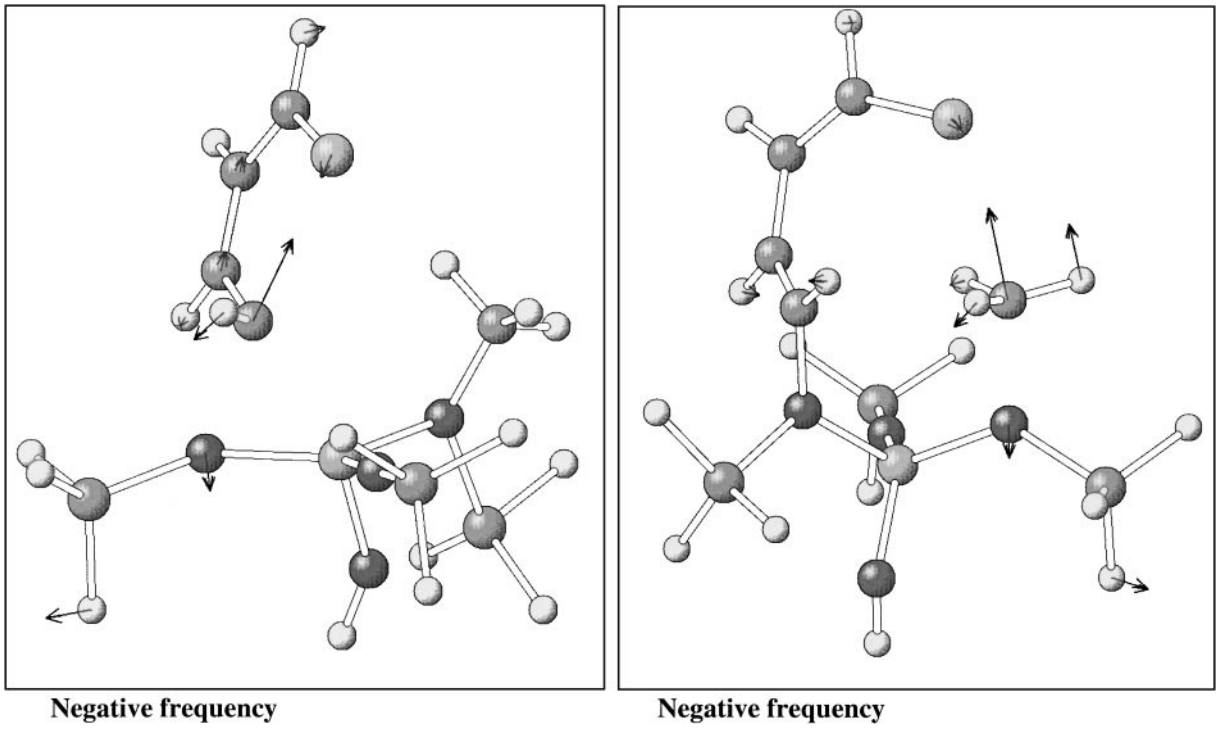

FIG. 5. Visualizations of the imaginary frequency involved in the thiophenic ring cracking transition state of thiophene catalyzed by an methyl alkoxide T_4 cluster (left) and of the imaginary frequency involved in the methylation mechanism of the consecutively formed species (right) (Reaction (4)).

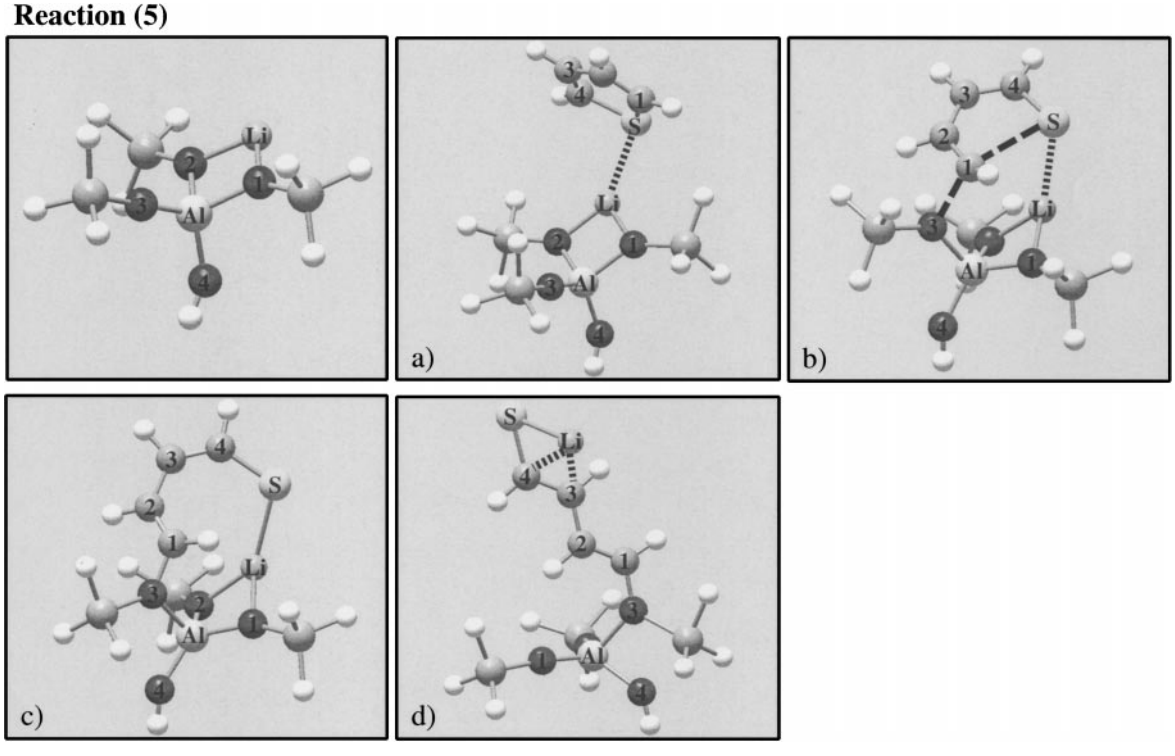

FIG. 6. Geometries of the intermediates (a, c, d) and transition state (b) of the cracking reaction of thiophene catalyzed by a Li^+-exchanged T_4 cluster $Al(OLiSiH_3)(OSiH_3)_2(OH)$ modeling the active site of a Li-exchanged zeolite catalyst (Reaction (5)).

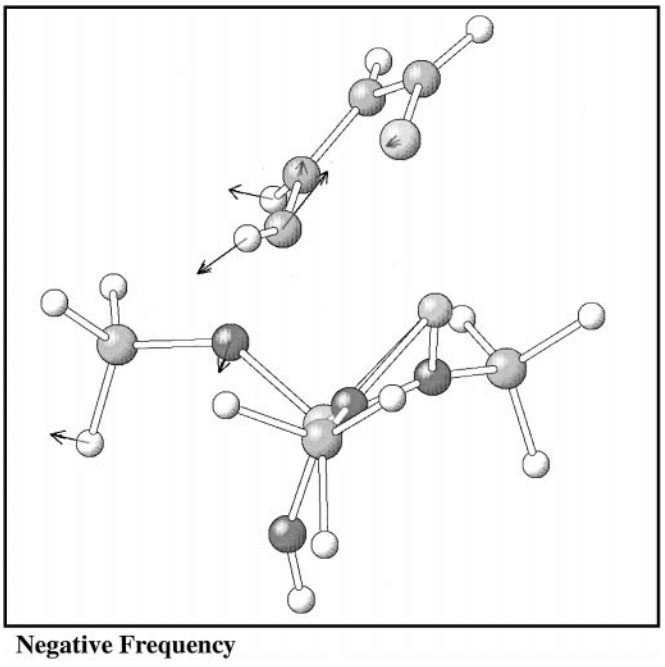

FIG. 7. Visualizations of the imaginary frequency involved in the thiophenic ring cracking transition state of thiophene catalyzed by a Li-exchanged T_4 cluster (Reaction (5)).

observations. The presence of H_2S, a product of the desulfurization reaction of thiophenic species, has been demonstrated to poison the reaction catalyzed by bifunctional catalysts (2, 10, 11). In the case of acid zeolite catalyzed reactions, a reversible deactivation has been observed (24). The presence of H_2O is even more problematic, and its presence is avoided in hydrotreatment reactions. It leads to a deactivation of the active sites and at high temperature to the destruction of the Brønsted sites (25).

However, H_2S and H_2O assist the mechanism in reducing the cracking step activation energy. One may also consider H_2O or H_2S adsorbed on the acidic site as the actual active site of the reaction.

The energy barriers reduce by 7 and 24 kJ/mol respectively for the mechanism step assisted by H_2S and H_2O. The orientation of the thiophenic ring in Reaction (6) and Reaction (7) is very similar to its orientation as observed in Reaction (3). The same may also be said for the deformation of the thiophenic ring (dihedral angle $SC_4C_2C_1$) when Reactions (1) and (3) and Reactions (6) and (7) are compared. After breaking of the thiophenic ring, the acidic proton jumps to S or O of the partner molecule. In return H_2S or H_2O loses one of its hydrogen atoms to the benefit of the consecutively negatively charged thiophene sulfur atom. The visualization of the TS imaginary frequency in both mechanisms (Fig. 9) shows that as in Reaction (1) hydrogen atoms are not involved in the thiophene cracking step. The frequencies of vibration of these hydrogen atoms seem rather to indicate that the protonation of thiophene sulfur via H_2O or H_2S follows "naturally" the cracking mechanism step and happens without a transition state.

The use of a coadsorbed molecule that helps the cracking mechanism step by avoiding distortion of thiophene and by favoring the protonation of thiophene sulfur allows a decrease of the activation barrier energy by ~20 kJ/mol. H_2S and H_2O have been used as models of assistant molecules. Song *et al.* (26) very recently observed that the presence of water increases significantly the rate of the cracking reaction of large polyaromatic compounds (coal). In order to allow this strong synergic effect of water, they used a reaction temperature lower than those used in the previous studies of these reactions. Even more recently, Ryder *et al.* (27) demonstrated for the zeolitic proton-exchange reaction that assisting molecules can affect considerably the rate of reaction. Reactions are affected even at very low loading of assisting molecules: water concentration below 1 ppm was enough to induce transition state assistance. Moreover, they have shown that the strongest impact of an assisting molecule occurs at low temperature.

3.3. Prehydrogenated Thiophene Cracking Reaction

In this section, we will study the cracking reaction of prehydrogenated thiophene molecules, viz. dihydrothiophene and tetrahydrothiophene (respectively Reaction (8) and Reaction (9), see Figs. 10 and 11 and Tables 1 and 4). The hydrotreatment reactions catalyzed by acidic zeolite usually take place in the presence of H_2. This H_2 helps to avoid coke

TABLE 4

Geometries of the Transition State Mechanisms for Reactions with an Assistant Molecule (H_2S and H_2O) as Labels Defined in Table 1[a]

Reaction (6)		Reaction (7)	
AlO_1	1.87	AlO_1	1.85
AlO_2	1.80	AlO_2	1.81
AlO_3	1.71	AlO_3	1.72
H_aS_1	2.15	H_aOw	1.40
S_1H_{s1}	1.41	O_wH_{w1}	1.00
$H_{s1}S$	2.29	$H_{w1}S$	2.19
C_1C_2	1.36	C_1C_2	1.36
O_1H_a	1.01	O_1H_a	1.06
SC_1	2.65	SC_1	2.62
SC_4	1.75	SC_4	1.77
C_1O_2	1.92	C_1O_2	1.94
SC_1O_2	164.9	SC_1O_2	163.3
AlO_2C_1	107.5	AlO_2C_1	109.0
C_1SC_4	81.4	C_1SC_4	81.8
$O_1H_aS_1$	177.0	O_1H_aOw	177.3
$S_1H_{s1}S$	169.7	$OwH_{W1}S$	175.9
$C_1C_2C_3C_4$	1.4	$C_1C_2C_3C_4$	2.9
$SC_4C_2C_1$	1.1	$SC_4C_2C_1$	0.4

[a] The atom labels are defined in the corresponding picture of the reactions (Fig. 8).

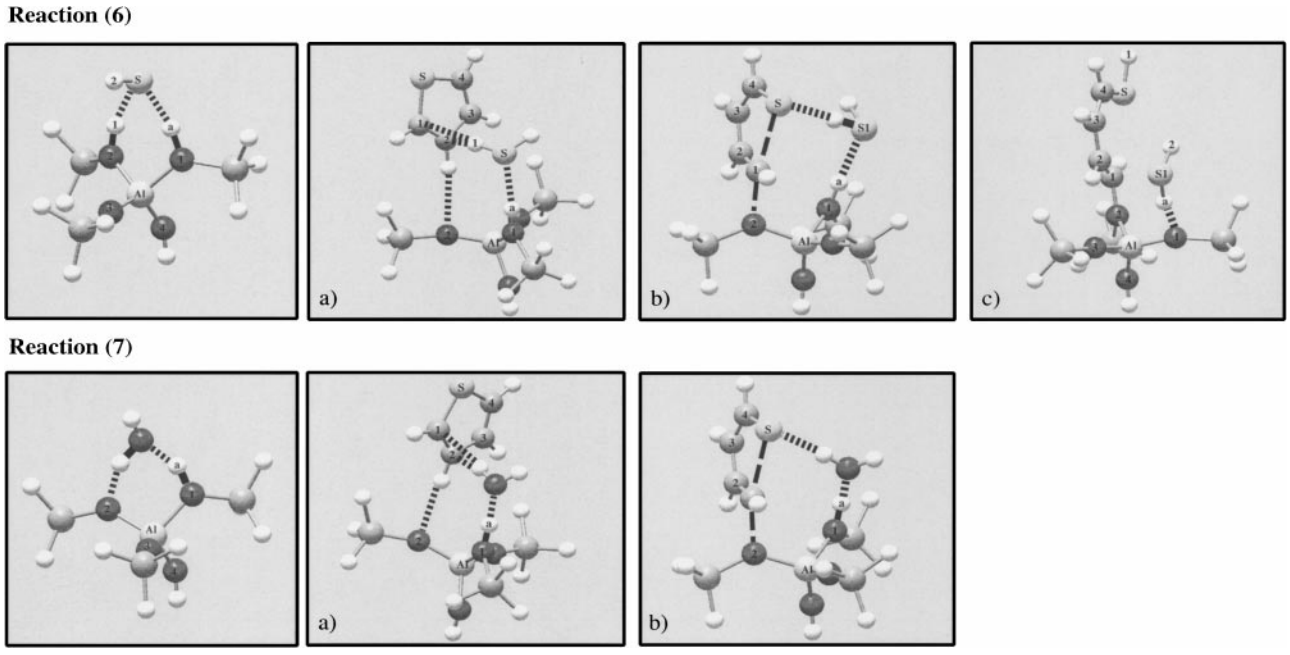

FIG. 8. Geometries of the intermediates (a, c) and transition state (b) of the cracking reaction of thiophene catalyzed by an acidic cluster and assisted by H_2S (top, Reaction (6)) and by H_2O (bottom, Reaction (7)). Left images are the geometries of adsorbed H_2S and H_2O interacting with the acidic site.

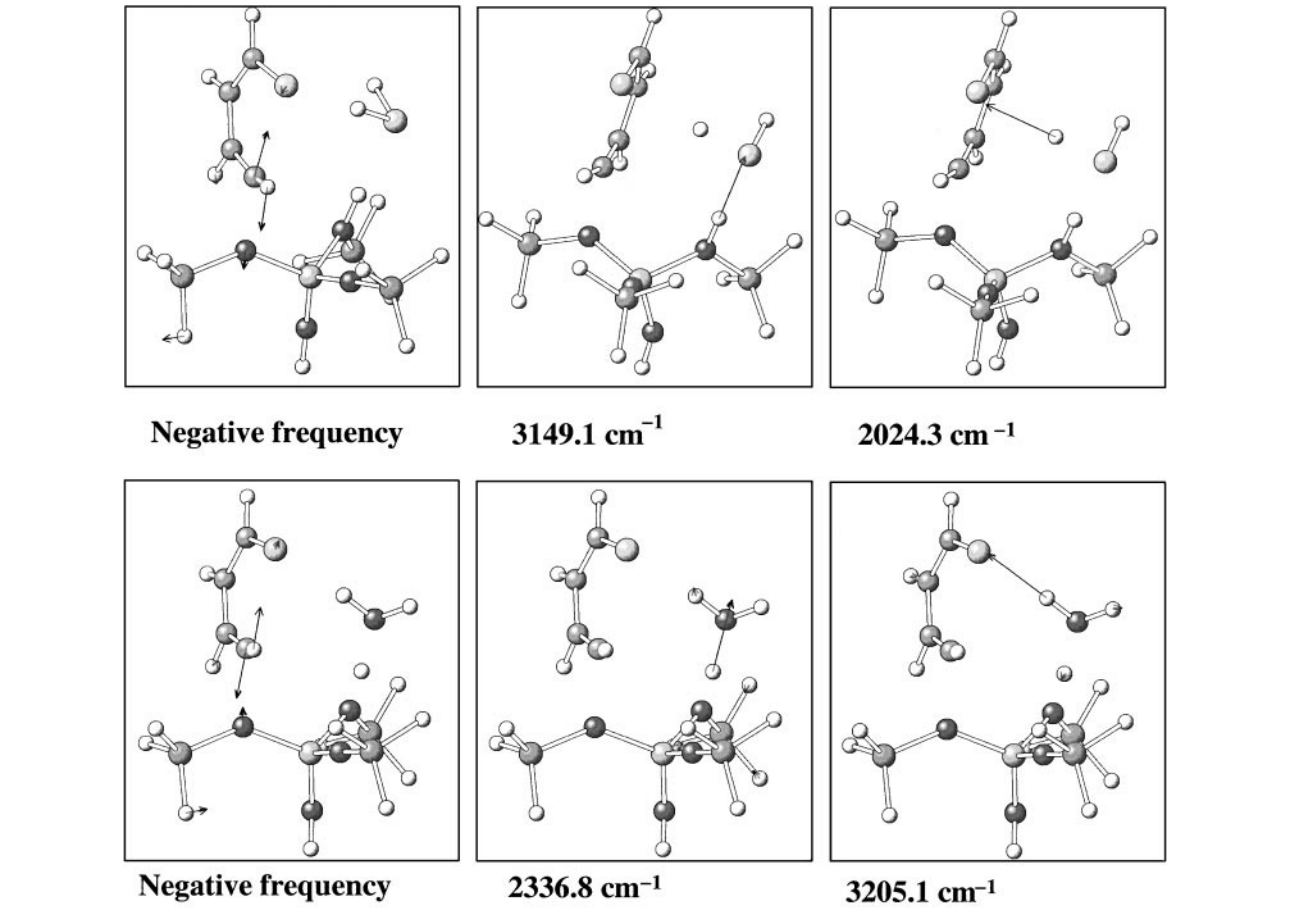

FIG. 9. Visualizations of the imaginary frequency involved in the thiophenic ring cracking transition state of thiophene catalyzed by an acidic T_4 cluster and assisted by H_2S (left top) and H_2O (left bottom) and of the two more intense frequencies of vibration of this transition state with their calculated values (in cm^{-1}) (middle and right).

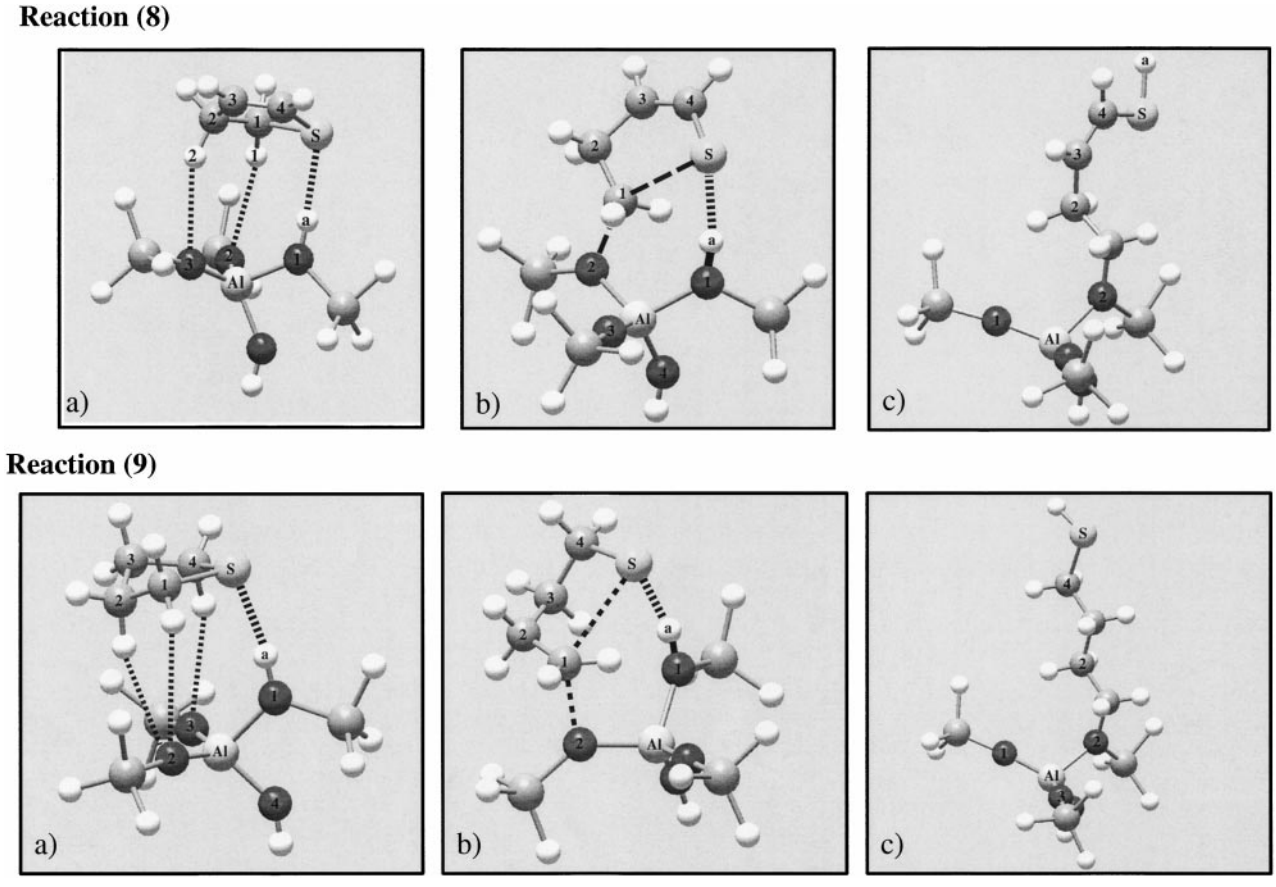

FIG. 10. Geometries of the intermediates (a, c) and transition state (b) of the cracking reactions of dihydrothiophene (top, Reaction (8)) and tetrahydrothiophene (bottom, Reaction (9)) catalyzed by an acidic cluster.

formation and the consecutive deactivation of the catalyst (8). Its presence as a mandatory reactant to perform the desulfurization of thiophene has been demonstrated (3). However, the introduction of H_2 gas in the processes has been shown to be partially useless: Bär *et al.* (28) demonstrated that only a small fraction of H_2 may actually participate in the reactions. The formation of H_2 from alkane catalyzed by acidic and bifunctional zeolite catalysts has been shown to greatly enhance the thiophene desulfurization reaction (12b). Yu *et al.* assumed that in this fashion the H_2 formed, in close proximity to the active sites, may be easily involved in later reactions. Only dihydrothiophene hydrogenated on C_1 and C_2 carbon atoms has been considered. The mechanism of the hydrogenation reaction of olefin catalyzed by acidic zeolite has been recently investigated in detail (29): the hydrogenation reaction occurs on two adjacent carbon atoms. Geobaldo *et al.* (30) showed that proton attack on the thiophene C_1 atom was most easily achieved in acidic zeolite.

The optimized geometry of adsorbed dihydrothiophene is similar to that of thiophene in that its S atom interacts with the acidic proton of the cluster (distances $H_aS = 2.22$ Å) (Reaction (8)). On the other hand, it is different in that two other physical bonds are formed: the hydrogen atoms of the sp^3 carbon atoms interact with the Lewis basic oxygen atoms (distances $H_1O_2 = 2.74$ Å and $H_2O_3 = 2.75$ Å). Its adsorption energy is -38 kJ/mol. More important to consider is that dihydrothiophene ring atoms are no longer coplanar. The dihydrothiophene molecule shows a higher distortion in order to adapt its geometry to the cluster one. This becomes clear when one considers the dihydrothiophene transition state geometry: the dihedral angle $C_1C_2C_3C_4$ is -25.4° and $SC_4C_2C_1$ is -26.3°. In return the distance H_aS is 2.14 Å, which is 0.19 Å smaller than in Reaction (1). The activation energy barrier decreases by 12 kJ/mol with respect to the thiophene cracking activation energy. Moreover, bond formation between a Lewis basic oxygen atom with an sp^3 carbon atom appears to be far more favorable than that with an sp^2 carbon atom: formation of the alkoxy species is 38 kJ/mol lower than in the case of the alkoxy species obtained with thiophene. This reduces strongly the possibility of the backward reaction mechanism.

Tetrahydrothiophene is strongly adsorbed on the cluster: three of its hydrogen atoms interact with Lewis basic oxygen

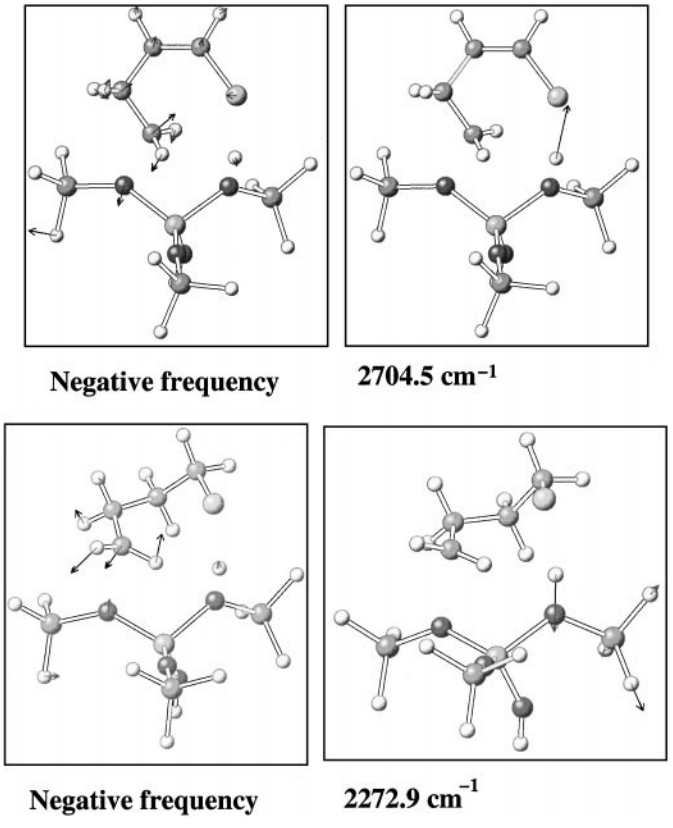

FIG. 11. Visualizations of the imaginary frequency involved in the thiophenic ring cracking transition state of dihydrothiophene (top left) and tetrahydrothiophene (bottom left) catalyzed by an acidic T_4 cluster and of the more intense frequency of vibration of the transition states of dihydrothiophene (top right) and tetrahydrothiophene (bottom right) with their calculated values (in cm^{-1}).

atoms ($H_1O_2 = 3.39$ Å, $H_2O_2 = 2.91$ Å, and $H_4O_3 = 2.85$ Å) and its sulfur atom interacts with the acidic proton ($H_aS = 2.16$ Å). The adsorption energy is $E_{ads} = -41$ kJ/mol. The sp^3 carbon atoms allow for a larger deformation of tetrahydrothiophene than dihydrothiophene or thiophene in the transition state geometry ($C_1C_2C_3C_4 = -66.2^\circ$ and $H_aS = 2.03$ Å). However, this does not lead to a decrease of the activation energy ($E_{act} = 237$ kJ/mol). This activation energy is higher than the activation energy barrier of thiophene cracking ($\Delta E_{act} = 11$ kJ/mol). Surprisingly, it appears that the tetrathiophene cracking reaction is more difficult to achieve than both dihydrothiophene and thiophene ones. In the case of dihydrothiophene, it is useful to analyze the thiophene species' geometries around the sulfur atom to understand this result. The distances are $SC_1 = 1.92$ Å and $SC_4 = 1.82$ Å whereas in the case of tetrahydrothiophene $SC_1 = SC_4 = 1.92$ Å for the adsorbed molecules on the acidic site. The dissymmetry that is shown by dihydrothiophene C_1SC_4 unit will favor cleavage of the SC_1 bond.

In the case of dihydrothiophene, prehydrogenation leads to a decrease of the activation barrier energy of the cracking reaction by approximately ~10 kJ/mol. This difference alone cannot explain the strongly enhanced experimental activity of cracking. The effect of prehydrogenation reactions of thiophene catalyzed by acidic zeolite has been shown to increase the yield of the reaction by a factor 10 (12c). Moreover, this prehydrogenation reaction affects considerably the alkoxy product: its energy decreases by ~40 kJ/mol compared with its equivalent in the case of thiophene cracking. These results are supported by the experimental observation that the main products of acid catalyzed thiophene cracking are but-1-ene and butane (6, 12b). Hydrogenation prior to cracking leads to a large stabilization of the product of this reaction.

4. CONCLUSIONS

In this theoretical study, we investigated the mechanisms involved in the cracking reaction of thiophene. We show that the Brønsted acidic site only indirectly participates in the controlling reaction. Considering these results one predicts that the acidity of zeolite catalyst is not a key factor (31). We demonstrated that even methyl alkoxy species or Li-exchanged zeolite can catalyze this reaction.

The use of a partner molecule (H_2O and H_2S) in order (i) to favor the protonation, (ii) to allow an easier protonation of the product of the cracking reaction, and (iii) to partly induce stronger Lewis basic behavior of catalytic oxygen atoms (20b) has been demonstrated to successfully decrease the cracking activation energy. However, experimentally H_2O and H_2S lead to a poisoning of the catalyst. In our study the coadsorption energy of thiophene and the partner molecule on the catalytically active site is similar to the adsorption energy of the partner molecule alone.

Finally, the effect of hydrogenation prior to cracking of thiophene has been investigated. Interestingly, the cracking reaction has not been shown to be dramatically favored (E_{act} decreases by ~10 kJ/mol). On the other hand, the effect on the product of the cracking reaction is very important. The stabilization of the alkoxy species product of the reaction is of the order of ~40 kJ/mol. Full prehydrogenation of thiophene to tetrahydrothiophene has not been shown to allow any amelioration of the cracking reaction rate compared to the dihydrothiophene case.

ACKNOWLEDGMENTS

This work has been performed within the European Research Group "Ab Initio Molecular Dynamics Applied to Catalysis," supported by the Centre National de la Recherche Scientifique (CNRS), the Institut Français du Pétrole (IFP), and the TotalFina Raffinage Distributions Co. X.R. thanks TotalFina Raffinage Distributions for the financial support. The authors thank P. Da-Silva from TotalFina, Centre Européen de Recherche et Technique, Procédés et Raffinage, for his fruitful comments. Computational resources were partly supplied by the Dutch National Computer Facilities.

REFERENCES

1. Knudsen, K. G., Cooper, B. H., and Topsøe, H., *Appl. Catal. A* **189**, 205 (1999).
2. (a) Sullivan, D. L., and Ekerdt, J. G., *J. Catal.* **178**, 226 (1998); (b) Miciukiewicz, J., Laniecki, M., and Domka, F., *Catal. Lett.* **51**, 65 (1998); (c) Zhang, Y., Wei, Z., Yan, W., Ying, P., Ji, C., Li, X., Zhou, Z., Sun, X., and Xin, Q., *Catal. Today* **30**, 135 (1996); (d) Logan, J. W., Heiser, J. L., McCrea, K. R., Gates, B. D., and Bussel, M. E., *Catal. Lett.* **56**, 165 (1998); (e) Kabe, T., Qian, W., Wang, W., and Ishihara, A., *Catal. Today* **29**, 197 (1996); (f) Bianchini, C., and Meli, A., *in* "Transition Metal Sulphides, Chemistry and Catalysis" (T. Weber, R. Prins, and R. A. van Santen, Eds.), NATO ASI Series 3, Vol. 60, p. 129. Kluwer Academic Publishers, Dordrecht, 1998.
3. Saintigny, X., Van Santen, R. A., Clémendot, S., and Hutschka, F., *J. Catal.* **183**, 107 (1999).
4. (a) Kramer, G. J., De Man, A. J. M., and Van Santen, R. A., *J. Am. Chem. Soc.* **113**, 6435 (1991); (b) Kramer, G. J., and Van Santen, R. A., *J. Am. Chem. Soc.* **115**, 2887 (1993); (c) Rigby, A. M., Kramer, G. J., and Van Santen, R. A., *J. Catal.* **170**, 1 (1997); (d) Van Santen, R. A., and Kramer, G. J., *Chem. Rev.* **3**, 637 (1995); (e) Frash, M. V., and Van Santen, R. A., *Topics Catal.* **9**, 191 (1999); (f) Van Santen, R. A., *J. Mol. Catal. A* **115**, 405 (1997); (g) Van Santen, R. A., *Catal. Today* **30**, 377 (1997).
5. Garcia, C. L., and Lercher, J. A., *J. Mol. Struct.* **293**, 235 (1993).
6. (a) Welters, W. J. J., De Beer, V. H. J., and Van Santen, R. A., *Appl. Catal. A* **119**, 253 (1994); (b) Welters, W. J. J., Vorbeck, G., Zandberger, H. W., De Haan, J. W., De Beer, V. H. J., and Van Santen, R. A., *J. Catal.* **150**, 155 (1994).
7. (a) Venuto, P. B., *Microporous Matter.* **2**, 297 (1994); (b) Hölderich, W. F., and Van Bekkum, H., *in* "Introduction to Zeolite Science and Practice" (H. van Bekkum, E. M. Flaningen, and J. C. Jansen, Eds.), Vol. 58, p. 631. Elsevier, Amsterdam, 1991.
8. Maxwell, I. E., and Stork, W. H. J., *in* "Introduction to Zeolite Science and Practice" (H. van Bekkum, E. M. Flaningen, and J. C. Jansen, Eds.), Vol. 58, p. 571. Elsevier, Amsterdam, 1991.
9. (a) Singhal, G. H., Espino, R. L., and Sobel, J. E., *J. Catal.* **67**, 446 (1981); (b) Vasudevan, P. T., and Fierro, J. L. G., *Catal. Rev.-Sci. Eng.* **38(2)**, 161 (1996).
10. (a) Muralidhar, G. ; Massoth, F. E., and Shabtai, J., *J. Catal.* **85**, 44 (1984); (b) Cid, R., Orellana, F., and Agudo, A. L., *Appl. Catal.* **32**, 327 (1987); (c) Laniecki, M., and Zmierczak, W., *Zeolites* **11**, 18 (1991).
11. (a) Landau, M. V., *Catal. Today* **36**, 393 (1997); (b) Michaud, P., Lemberton, J. L., and Pérot, G., *Appl. Catal. A* **169**, 343 (1998).
12. (a) Landau, M. V., Berger, D., and Herskowitz, M., *J. Catal.* **158**, 236 (1996); (b) Meille, V., Schulz, E., Lemaire, M., and Vrinat, M., *J. Catal.* **170**, 29 (1997); (c) Yu, S. Y., Li, W., and Iglesia, E., *J. Catal.* **187**, 257 (1999).
13. Eichler, U., Brändel, M., and Sauer, J., *J. Phys. Chem, B* **101**, 10035 (1997).
14. (a) Blaszkowski, S. R., and Van Santen, R. A., *in* "Transition State Modeling for Catalysis" (D. G. Truhlar and K. Morokuma, Eds.), ACS Symposium Series 721, Chapter 24, Am. Chem. Soc., Washington, DC, 1999; (b) Van Santen, R. A., and Rozanska, X., *in* "Advances of Chemical Engineering," Academic Press, to appear.
15. (a) Sauer, J., Sierka, M., and Haase, F., *in* "Transition State Modeling for Catalysis" (D. G. Truhlar and K. Morokuma, Eds.), ACS Symposium Series 721, Chapter 28, Am. Chem. Soc., Washington, DC, 1999; (b) Vollmer, J. M., and Truong, T. N., *J. Phys. Chem. B* **104**, 6308 (2000); (c) Zygmunt, S. A., Curtiss, L. A., Zapol, P., and Iton, L. E., *J. Phys. Chem. B* **104**, 1944 (2000).
16. (a) Sinclair, P. E., De Vries, A., Sherwood, P., Catlow, C. R. A., and Van Santen, R. A., *J. Chem. Soc., Faraday Trans.* **94**, 3401 (1998); (b) Boronat, M., Zicovich-Wilson, C. M., Corma, A., and Viruela, P., *Phys. Chem. Chem. Phys.* **1**, 537 (1999).
17. Frisch, M. J., Trucks, G. W., Schlegel, H. B., Scuseria, M. A., Robb, M. A., Cheeseman, J. R., Zakrzewski, V. G., Montgomery, J. A., Stratmann, R. E., Burant, J. C., Dapprich, S., Millam, J. M., Daniels, A. D., Kudin, K. N., Strain, M. C., Farkas, O., Tomasi, J., Barone, V., Cossi, M., Cammi, R. ; Mennucci, B., Pomelli, C., Adamo, C., Clifford, S., Ochterski, J., Petersson, G. A., Ayala, P. Y., Cui, Q., Morokuma, K., Malick, D. K., Rabuck, D. K., Raghavachari, K., Foresman, J. B., Cioslowski, J., Ortiz, J. V., Stefanov, B. B., Liu, G., Liashenko, A., Piskorz, P., Komaromi, I., Gomperts, R., Martin, R. L., Fox, D. J., Keith, T., Al-Laham, M. A., Peng, C. Y., Nanayakkara, A., Gonzales, C., Challacombe, M., Gill, P. M. W., Johnson, B. G., Chen, W., Wong, M. W., Andress, J. L., Head-Gordon, M., Replogle, E. S., and Pople, J. A., Gaussian 98, revision A. 1. Gaussian, Inc., Pittsburg PA, 1998.
18. (a) Becke, A. D., *Phys. Rev. A* **38**, 3098 (1988); (b) Lee, C., Yang, W., Parr, R. G., *Phys. Rev. B* **37**, 785 (1988); (c) Becke, A. D., *J. Chem. Phys.* **98**, 5648 (1993).
19. Zygmunt, S. A., Mueller, R. M., Curtiss, L. A., and Iton, L. E., *J. Mol. Struct.* **430**, 9 (1998).
20. (a) Boys, S. F., and Bernardi, F., *Mol. Phys.* **19**, 553 (1970); (b) Van Duijneveldt, F. B., *in* "Molecular Interactions: From Van der Waals to Strongly Bound Complexes" (S. Scheiner, Ed.), p. 81. Wiley, New York, 1997; (c) Lendvay, G., and Mayer, I., *Chem. Phys. Lett.* **297**, 365 (1998).
21. Civalleri, B., Garrone, E., and Ugliengo, P., *J. Phys. Chem. B* **102**, 2373 (1998).
22. Ono, Y., *in* "Catalysis by Zeolites" (B. Imelik, C. Naccache, Y. Ben Taarit, J. C. Vedrine, G. Coudurier, and H. Praliaud, Eds.), p. 19. Elsevier, Amsterdam, 1980.
23. Paukshtis, E. A., Malysheva, L. V., and Stepanov, V. G., *React. Kinet. Catal. Lett.* **65**, 145 (1998).
24. (a) Thomazeau, C., Canaff, C., Lemberton, J. L., and Guisnet, M., *Appl. Catal. A* **103**, 163 (1993); (b) Sárkány, J., *Appl. Catal. A* **188**, 369 (1999).
25. Guisnet, M., and Magnoux, P., *Catal. Today* **36**, 477 (1997).
26. Song, C., Daini, A. K., and Yoneyama, Y., *Fuel* **79**, 249 (2000).
27. Ryder, J. A., Chakraborty, A. K., and Bell, A. T., *J. Phys. Chem. B* **104**, 6998 (2000).
28. Bär, N.-K., Ernst, H., Jobic, H., and Kärger, J., *Magn. Reson. Chem.* **37**, 579 (1999).
29. Senger, S., and Radom, L., *J. Am. Chem. Soc.* **122**, 2613 (2000).
30. Geobaldo, F., Palomino, G. T., Bordiga, S., Zecchina, A., and Areán, C. O., *Phys. Chem. Chem. Phys.* **1**, 561 (1999).
31. Serrano, D. P., Aguado, J., and Escola, J. M., *Ind. Eng. Chem. Res.* **39**, 1177 (2000).